Applied Mathematical Modelling 39 (2015) 2416–2435

Contents lists available at ScienceDirect

Applied Mathematical Modelling

journal homepage: www.elsevier.com/locate/apm

The influence of the multiplicity of infection upon the dynamics of a crop-pest–pathogen model with defence mechanisms

Hong Zhang [a], Paul Georgescu [b,*]

[a] Department of Financial Mathematics, Jiangsu University, ZhenJiang, JiangSu 212013, PR China
[b] Department of Mathematics, Technical University of Iaşi, Bd. Copou 11, 700506 Iaşi, Romania

ARTICLE INFO

Article history:
Received 31 October 2012
Received in revised form 8 May 2014
Accepted 7 November 2014
Available online 20 November 2014

Keywords:
Pest control
Defence mechanisms
Evolutionary response
Multiplicity of infection
Stability analysis

ABSTRACT

To prevent pest outbreaks, growers often resort to the release of insect-pathogenic viruses rather than to the use of pesticides, which threaten human health and adversely impact the environment. One of the unfortunate consequences of this approach, however, is the onset of resistance mechanisms in pests. In this paper, we propose a model which couples the analysis of the within-pest virus dynamics and the investigation of the evolutionary response of defence mechanisms. The ecosystem consisting in the soybean crop and its major pest, the fourth instar larvae of *Spodoptera litura*, which is infected by *Spodoptera polyhedrosis* viral particles, is used as our main example. Five types of resistance mechanisms are investigated, each expressing resistance through one or more model parameters. By means of linearization, phase field analysis and numerical simulations, we illustrate and analyze the stability of the steady states of our model. Moreover, we use a graph representing the values of the function of the lifetime reproductive success of the mutant in the resident pest population at equilibrium states to find which are the best and the worst pest control strategies. Our findings show the impact of evolutionary resistance on the selection for the multiplicity of infection of the within-pest virus, in the sense that to establish the viral infection there is a threshold of the mutant trait.

1. Introduction

Insect pests outbreaks, which threaten the supply of food and its quality, have always been major concerns for farming communities. Although chemical insecticides are easy to apply, their use may be detrimental in the long run for both humans and environment [1]. Biological controls, which represent an important alternative to chemical insecticides, can then be employed, leading to less adverse effects. Insects, like humans and other animals, can be infected by pathogenic organisms such as bacteria, viruses, fungi and protozoa [2] that either incapacitate them or interfere with their biological processes [3–9], being generally compatible with other natural enemies.

Baculoviruses are naturally occurring insect pathogens that can be used as biological control agents to control pest insects [10]. A field survey using the virus *Spodoptera polyhedrosis* against the fourth instar larvae of *Spodoptera litura* has been carried out by Prasad and Wadhwani [11] and is outlined as follows. The viral preparation contained 2×10^9 polyhedra per ml. Considering this as stock solution, four different dilutions were prepared and fed to the target pest population by leaf-dip method [12]. The polyhedra were taken up orally by the larvae together with the leaf. After ingestion, the polyhedra

* Corresponding author.
E-mail addresses: hongzhang@ujs.edu.cn (H. Zhang), v.p.georgescu@gmail.com (P. Georgescu).

http://dx.doi.org/10.1016/j.apm.2014.11.008
0307-904X/

dissolved under the alkaline conditions in the midgut. The nucleocapsids were then released and consequently severely affected the midgut epithelial cells [13]. In the nucleus of these cells virus replication took place, budded viruses were produced in the late stages and then the occlusion bodies were produced in the final stage, the envelope being acquired from host cell nucleus and embedded in the matrix of occlusion body protein. These occlusion bodies were released when cells lysed to further spread baculovirus infection to next host. After infecting the larval midgut tissues, the budded virus particles entered the haemocoel, through which the virus invaded various tissues. Consequently, the histomicrograph clearly revealed that various midgut cells, fat bodies, connective tissues and integument either lost their identity or became highly disorganized [11].

The overall destruction of tissues led to the apparition of liquefied contents inside the body cavity, giving the infected insect a turgid appearance. The infected larval bodies were laden with polyhedral occlusion bodies (POBs) containing viral particles. Even a slight damage or disturbance of the integument releases liquefied body fluids containing large numbers of POBs. This infected fluids further spread infection when healthy larvae came in contact with it [14–16].

Given the rapid evolutionary changes in the pest population, it is not surprising that control agents are sometimes rendered ineffective, due to the natural evolutionary response to the environmental stress. This has been observed in [17–19] for Indian meal moth, *Plodia interpunctella*; American bollworm of cotton, *Heliothis virescens*; beet armyworm, *Spodoptera exigua*, and tobacco caterpillar, *Spodoptera litura*, which have all shown different degrees of resistance to *Bacillus thuringiensis* and insect viruses. Although significant efforts have been put into designing programmes of pesticide usage which avoid pesticide resistance, a more realistic goal is to delay the onset of resistance to pesticides, that is, to "mitigate resistance" [20].

Compared to vertebrates, insects do not possess the ability to produce antibodies against foreign antigens, and hence cannot release alpha/beta interferons in response to viral infections. Nevertheless, the defence mechanisms of insects can be classified into two broad groups. The first group consists of structural and passive barriers such as cuticle, gut physicochemical properties and peritrophic membrane, that is, of non-specific mechanisms. The second one consists of specific defence mechanisms, including cellular and humoral immunity, and inhibitors of apoptosis. Specifically, cellular responses involve phagocytosis, nodulation and encapsulation, humoral reactions include activation of prophenoloxidase (ProPO) cascade and induction of immune proteins like lysozymes, lectins and antibacterial and antifungal proteins [21,22], and inhibitors of apoptosis (IAP) are a family of functionally and structurally related proteins, which serve as endogenous inhibitors of programmed cell death.

In recent decades, besides investigations on the experimental and theoretical applications of microbial pathogens to suppress pests [4,23–28], many studies have attempted to formulate and analyze deterministic models of pest-pathogen dynamics [30–39], making use of analytic results to set up field experiments and to analyze their conclusions. To adequately incorporate the effects of the pathogens on the pest population, Anderson and May [32] investigated the pathogen–host model and showed that if the release rate exceeded a critical level, the host (pest) population would decrease to zero.

Resistance modeling usually takes one of the following two forms: (1) modeling the processes which take place within a single host, or (2) modeling the spread of resistance through a population of hosts [40]. However, both types are rarely combined, although exceptions do exist [41,42]. Modeling within-host bacterial dynamics or within-ecosystem dynamics in insect populations is usually accomplished using ordinary differential equations. Examples of models of this type include those of [43–46]. The models describing the spread of resistance factors through a population of hosts usually follow the SIS models; see, for instance, studies on the epidemiology of resistance spread [47,48]. Further, [42] explored both of the above situations in a model that incorporates within-host dynamics and tracks the average infection rates across hosts, pointing out that indiscriminate use of antibiotics greatly increases the rate of defence development. [41] provided another excellent modeling framework in which the direct interaction of hosts is considered, rather than interaction through an environmental pool, and found that resistance can be managed by cycling different antibiotics or using combinations of antibiotics.

On the other hand, of all physical parameters tested for in vitro baculovirus infection, the multiplicity of infection was found as being the most important factor to influence the total percentage of infected cells [49]. However, in the above-mentioned models, the authors ignored the effect of defence mechanisms upon the variation of the viral multiplicity of infection of cells within infected insects.

The aim of this paper is to introduce a model of a pest management strategy which accounts for defence responses depending upon a variable multiplicity of infection (MOI). The latter is understood as the number of viruses that are added per cell during infection [50], in response to pest control measures. In this regard, the MOI is highly relevant for understanding the virus dynamics and its evolution. Obviously, mixed genotype infections can occur only if the MOI is > 1, while recombination or complementation between different genotypes can occur only in mixed-genotype infected cells. Also, higher MOI raises the ploidy, partially masking deleterious variants. This reduces the deterministic forces by which these deleterious variants are removed by natural selection, maintaining a greater genetic diversity and thereby increasing the pool for recombination or complementation, possibly for longer periods of time [51,52]. In turn, rapid evolution during periods of high MOI may generate new viral strains. Lower ($\leqslant 1$) MOI levels relax selection between virus genotypes at the within-cell level, since virions rarely have to share a cell, increasing the competition at higher levels (within-tissue, within-host, between-host). That is, MOI is relevant not only for phenomena which occur at the cellular level, but also for the viral evolution at higher levels.

An extensive spatio-temporal monitoring of the cellular MOI of a eukaryotic virus, the *Cauliflower mosaic virus* (CaMV), from the onset of the systemic invasion until the senescence of its host plant, has been performed in [53], wide variations

throughout a single infection being observed, with values starting close to 2 and increasing up to 13 before decreasing to initial levels in the latest infection stages. This establishes MOI as an evolving trait, being suggested in [53] that a possible explanation for this behavior would be a host developmental or physiological effect on the MOI, related to the previously described impairment of virus infection upon flowering, or to the onset of a plant defense mechanism, with a resulting drop in viral load.

We restricted our investigation to the study of a single variable virus trait, the MOI, which indicates that our conclusions are valid only for the variation of this trait. Moreover, within-pest virus dynamics at the organ cell level and within-ecosystem disease dynamics are considered. We intend to determine not only the best strategy through which the mutant can establish the viral infection in the pest but also the worst scenario, in which the mutant can not establish the viral infection in the pest regardless of the defence response.

Our approach relies on stability analysis, phase field analysis, numerical simulations of ODEs and the theory of evolutionary analysis, as introduced in [54]. Although our model is of a generic nature, we had in mind the biosystem represented by soybean biomass and its pest, the fourth instar larvae of *Spodoptera litura* [55], because the gathering larvae after third instar turn to gluttony period [29], infected by *Spodoptera polyhedrosis* viral particles [56], as our main example.

2. The model

The baculovirus life cycle involves two distinct forms of virus, occlusion body-derived virions (ODVs) and budded virions (BVs), with distinct enveloped origins and compositions [57]. ODVs play important roles in the insect-to-insect transmission of viruses through oral infection, while BVs have been shown to be essential for cell-to-cell transmission within infected insects [14,15]. In the following, we shall consider a model which couples the analysis of the within-pest virus dynamics and the investigation of the variable response of defence mechanisms.

2.1. Crop-pest-POBs dynamics: the model

Our population model describes the time-dependent variation of the biomass of the soybean crop $C(t)$, of the density of its major pest and of the density of the POBs containing viral particles. It is assumed that in the absence of larvae, the soybean biomass obeys a logistic growth law [58] with intrinsic growth rate r and carrying capacity $K = \frac{r}{\kappa}$. Healthy larvae are infected by ODVs and consequently the pest population may be divided into healthy, $P_H(t)$, and infected, $P_I(t)$, subgroups. Also, one assumes that only the healthy larvae are capable of predation, modeled by a Holling type II functional response $\frac{aC(t)}{b+C(t)}$. We assume that the feeding on foliage contaminated with the occluded form of the virus, $W(t)$, of the healthy insects is random and consequently the interaction between them is characterized by a simple mass action incidence with constant transmission coefficient β [59]. Ideally, the transmission of infection term $\beta P_H(t)W(t)$ should also depend on the density of the soybean biomass $C(t)$, since when the infected insect dies and "melts" away or falls apart on foliage, it releases more POBs, which are then ingested by the healthy larvae with the foliage. That is, the transmission term implicitly depends on the availability of foliage. However, to obtain a more mathematically tractable problem, we have assumed that the transmission of the disease occurs faster than the variations in the density of the soybean biomass, which allows us to consider the transmission coefficient β as being a constant. Note that considerations leading to the fact that nuclear polyhedrosis virus transmission in gipsy moths is a nonlinear function of virus density are given in [60]. For the sake of convenience, we do not consider stage structures in any population, but we do consider the immigration of healthy larvae from outside, at a constant rate. The model can then be given in the form

$$\frac{dC(t)}{dt} = rC(t)\left(1-\frac{C(t)}{K}\right) - \frac{aC(t)P_H(t)}{b+C(t)} - hC(t) = (r-h)C(t) - \kappa C(t)^2 - \frac{aC(t)P_H(t)}{b+C(t)}, \tag{1}$$

$$\frac{dP_H(t)}{dt} = A + \frac{acC(t)P_H(t)}{b+C(t)} - \beta P_H(t)W(t) - d_P P_H(t), \tag{2}$$

$$\frac{dP_I(t)}{dt} = \beta P_H(t)W(t) - (d_P+\epsilon)P_I(t), \tag{3}$$

$$\frac{dW(t)}{dt} = eP_I(t) - d_W W(t), \tag{4}$$

in which the state variables and parameter values are listed in Table 1, and for which the flow diagram is given by Fig. 1(a). Since the mortality in infected larvae is nearly 100% and the horizontal transmission of baculoviruses is by the release of occlusion bodies from the liquefied cadavers of dead larvae (note that baculoviruses are obligate host-killing microparasites), it is then assumed that the POBs yield is proportional to the density of infected larvae with a proportionality constant e, and that d_W represents their removal rate. From a biological point of view, several assumptions upon the values of the parameters of the model are listed as follows.

(a) The disease-related death rate is much higher than the natural death rate, that is, $\epsilon \gg d_P$;
(b) The intrinsic growth rate of the crop is higher than its harvest rate, that is, $r > h$;
(c) The total fertility rate of the uninfected larvae is higher than their natural mortality rate, that is, $ac > d_P$.

Table 1
State variables and parameters of the model (Values of the parameters and initial state variables used in the following simulations).

Symbol	Quantity	Default value	Dimensions	Sources
C	Biomass of the soybean crop population	Variable	gram m^{-2}	
P_H	Density of the healthy pest population	Variable	pest m^{-2}	
P_I	Density of the infected pest population	Variable	pest m^{-2}	
W	Density of the POBs	Variable	polyhedron ml^{-1}	
V	Concentration of viruses	Variable	viruses ml^{-1}	
C_U	Amount of uninfected cells	Variable	cells ml^{-1}	
C_I	Amount of infected cells	Variable	cells ml^{-1}	
r	Crop intrinsic growth rate	0.45	day^{-1}	[72]
K	Carrying capacity of the soybean crop	900	gram m^{-2}	
a	Predation rate of susceptible pests	0.1	gram $pest^{-1}$ day^{-1}	
b	Half saturation constant of susceptible pests	100	gram m^{-2}	
c	Reproductive rate of susceptible pests	0.5	pest $gram^{-1}$	
h	Harvest rate of the crop	–	day^{-1}	
d_P	Natural death rate of pests	0.01	day^{-1}	
e	Production rate of the POBs	–	polyhedron m^2 $pest^{-1}$ ml^{-1} day^{-1}	
d_W	Removal rate of the POBs	0.6	day^{-1}	
ϵ	Disease-related death rate	–	day^{-1}	
β	Transmission coefficient	–	ml $polyhedron^{-1}$ day^{-1}	
A	Immigration rate of susceptible pests	–	pest m^{-2} day^{-1}	
$\mu_{\max}$	Maximal production rate of healthy cells	0.624	day^{-1}	[65]
$C_{\max}$	Maximal cell concentration	1.2×10^6	cells ml^{-1}	[73]
d_C	Natural death rate of uninfected cells	0.018	day^{-1}	[65]
d_V	Death rate of infected cells	–	day^{-1}	
γ	Contact rate	2×10^{-10}–2×10^{-9}	ml $virus^{-1}$ day^{-1}	[65]
V_0	Dilution rate of viruses	–	day^{-1}	
F	Degraded rate of viruses	0.35	day^{-1}	
k_{va}	Viral attachment rate	–	viruses $cell^{-1}$	
N	Average viral burst size	500	viruses $cell^{-1}$	[73]
m	Multiplicity of infection (MOI)	0.01–20		[69,50]
α	Scaling constant	0.9		

"–" represents that, in the following sections, the relationship between the values of these parameters and dynamics of the system will be surveyed in detail.

2.2. Within-pest virus dynamics: the model

The flow diagram in Fig. 1(b) will be used to describe the cell-to-cell transmission within infected insects [14,15]. For simplicity, the model for the within-pest virus dynamics describes only the basic interactions among uninfected host cells $C_U(t)$, infected host cells $C_I(t)$ and budded viruses $V(t)$ in vital organs. Also, for sake of convenience, we thereby did not consider the delays due to cell division or differentiation.

Following the modeling ideas introduced in [61–63], we assume that the amount of healthy cells increases with a specific cell growth rate $\mu_{\max}\frac{C_{\max}-(C_U(t)+C_I(t))}{C_{\max}}$ which is, in principle, independent of the virus titre, in which $\mu_{\max}$ is the maximal cell growth rate, and $C_{\max}$ is the maximal cell concentration due to cell growth inhibition on confluent microcarriers. Each uninfected cell has a constant probability per time unit to die, denoted by d_C. Using again the simple mass action incidence assumption, we find the removal rate of healthy cells to be $\gamma C_U(t)V(t)$, in which γ is the virus infection rate. We hereby consider that a proportional rate V_0 accounts for the dilution rate of viruses, when swallowed and then absorbed in the haemocoel, since insects have developed responses and barriers to combat baculovirus infection [64]. For the sake of simplicity, we assume that the absorbtion process is modeled by a linear law.

It is fairly evident that infected cells eventually lyse, which leads to a mortality rate d_V, and then release budded viruses at a specific rate $d_V N\alpha$. In general, d_V depends on the MOI m [65]. The parameter N is the average viral burst size for the total infected cell population. Note that N is a constant in the limit case in which the burst size is independent of the multiplicity of infection [65], and the parameter α is necessarily considered as a scaling constant because not every virion is infectious [66]. On the other hand, released viruses are either degraded at a specific rate F, or attached to receptor site on the susceptible cell wall with a specific attachment rate k_{va}. Moreover, k_{va} should depend on m since the MOI refers to a group of cells inoculated with infectious virus particles. Finally, it is assumed that the outflow contains only viral particles and does not contain any organ cells. Assuming all the above, the model can be given in the following form

$$\frac{dC_U(t)}{dt} = \mu_{\max}C_U(t)\frac{C_{\max}-(C_U(t)+C_I(t))}{C_{\max}} - d_C C_U(t) - \gamma C_U(t)V(t), \tag{5}$$

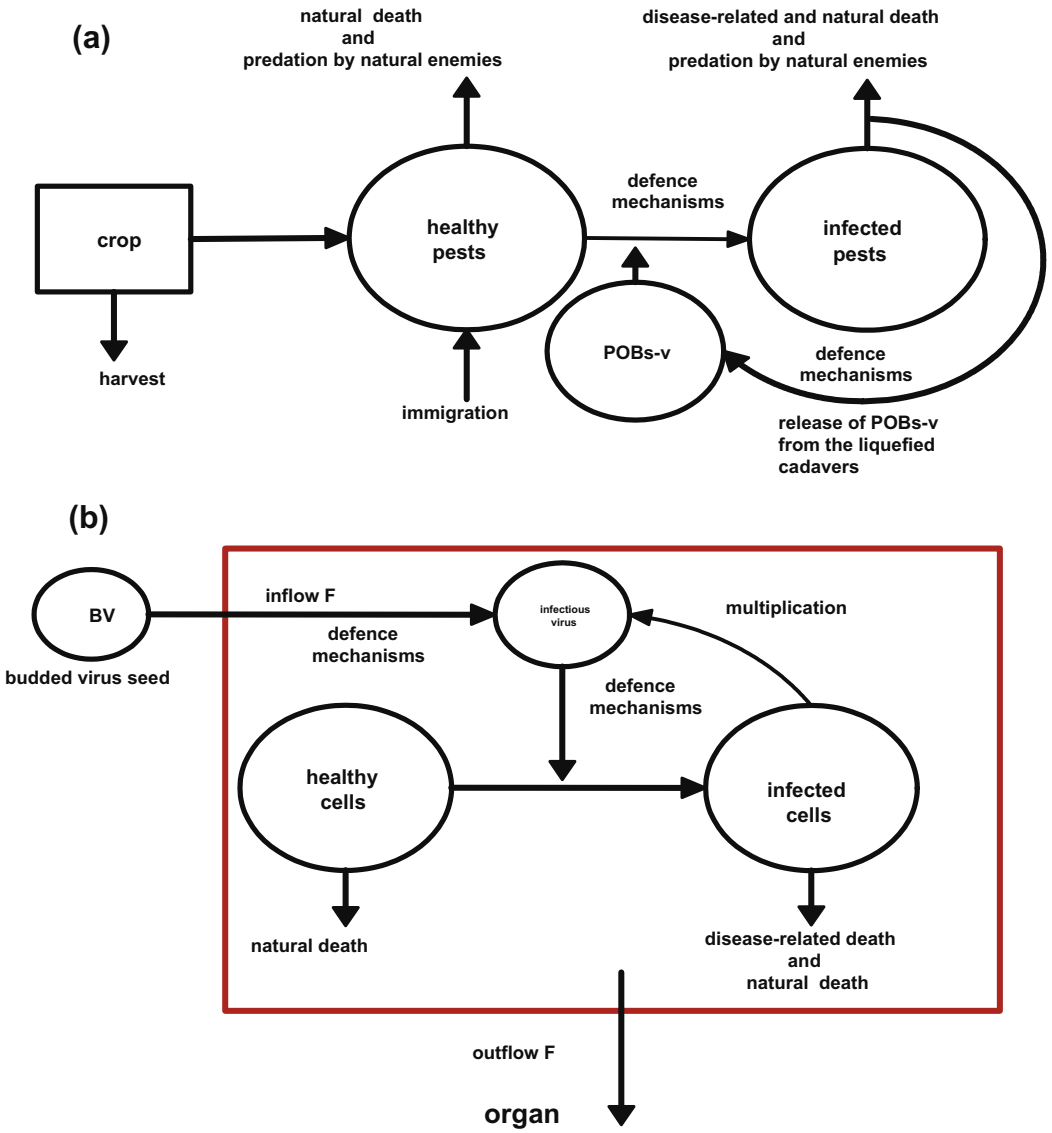

Fig. 1. (a) A schematic illustration of the crop-pest-POBs model, including possible defence mechanisms. (b) A graphical representation of the within-pest virus dynamics, including possible defence mechanisms. V represents the viral particles.

$$\frac{dC_I(t)}{dt} = \gamma C_U(t)V(t) - d_V C_I(t), \tag{6}$$

$$\frac{dV(t)}{dt} = d_V N\alpha C_I(t) - (F - V_0)V(t) - k_{va}\gamma C_U(t)V(t), \tag{7}$$

where the state variables and the parameter values used in our model are listed in Table 1. Here $d_V = d_V(m)$ and $k_{va} = k_{va}(m)$ are increasing with respect to the value of the MOI. From a biological point of view, several assumptions upon the values of the parameters of the model are listed as follows.

(a) The removal rate of infected cells is much higher than the natural death rate of uninfected cells, that is, $d_V \gg d_C$;
(b) The maximal cell concentration is larger than the natural death rate of uninfected cells, that is, $\mu_{\max} > d_C$;
(c) The yield of virus particles per infected cell is higher than the viral attachment rate, that is, $\alpha N > k_{va}$;
(d) The clearance rate of viruses, F, is higher than its absorbtion rate, V_0, that is, $F > V_0$.

2.3. Crop-pest-POBs dynamics: analytic findings

To pursue the dynamical analysis of the crop-pest-POBs model, we first summarize all possible semi-trivial steady states, listed in Table 2, together with some information about their stability.

The armyworm larvae can be infected by baculoviruses. In the initial stages of the epidemic, we can assume that P_H is near the disease-free equilibrium value P_H^*, and approximate the last two Eqs. (3) and (4) for P_I and W with the linearized system

$$\begin{pmatrix} \frac{dP_I}{dt} \\ \frac{dW}{dt} \end{pmatrix} = \begin{pmatrix} 0 & \beta P_H^* \\ 0 & 0 \end{pmatrix} \begin{pmatrix} P_I \\ W \end{pmatrix} - \begin{pmatrix} d_P + \epsilon & 0 \\ -e & d_W \end{pmatrix} \begin{pmatrix} P_I \\ W \end{pmatrix}.$$

It follows from [67] that the matrix

$$\begin{pmatrix} \frac{e\beta P_H^*}{d_W(d_P+\epsilon)} & \frac{\beta}{d_W} \\ 0 & 0 \end{pmatrix}$$

has a single nonzero eigenvalue, which represents the basic reproduction number of the system, namely

$$\Re = \frac{e\beta P_H^*}{d_W(d_P+\epsilon)}.$$

When $\Re > 1$, the infection is able to spread in the pest population and it will be observed in what follows that the densities of soybean biomass, healthy larva, infectious larvae and POBs tend towards stable steady states. Let us denote

$$C_1^* = \frac{(r-h) - b\kappa + \sqrt{((r-h)-b\kappa)^2 + 4\kappa\left((r-h)b - \frac{ad_W(d_P+\epsilon)}{e\beta}\right)}}{2\kappa},$$

$$C_2^* = \frac{(r-h) - b\kappa - \sqrt{((r-h)-b\kappa)^2 + 4\kappa\left((r-h)b - \frac{ad_W(d_P+\epsilon)}{e\beta}\right)}}{2\kappa}$$

Let us also denote

$$A^* = \frac{(r-h)bc}{2} + bc\frac{\left(b\kappa + \sqrt{((r-h)-b\kappa)^2 + 4\kappa\left((r-h)b - \frac{ad_W(d_P+\epsilon)}{e\beta}\right)}\right)}{2} - \frac{d_W(d_P+\epsilon)(ac-d_P)}{e\beta}$$

$$A_* = \frac{(r-h)bc}{2} + bc\frac{\left(b\kappa - \sqrt{((r-h)-b\kappa)^2 + 4\kappa\left((r-h)b - \frac{ad_W(d_P+\epsilon)}{e\beta}\right)}\right)}{2} - \frac{d_W(d_P+\epsilon)(ac-d_P)}{e\beta}.$$

We consider the following cases:

Case I : If the harvest rate of the crop h satisfies

$$h \in \left(\max\left\{0, r - \frac{ad_W(d_P+\epsilon)}{be\beta}\right\}, \min\left\{r\left(1+\frac{b}{K}\right) - 2\sqrt{\frac{\kappa ad_W(d_P+\epsilon)}{e\beta}}, r\left(1-\frac{b}{K}\right)\right\}\right)$$

Table 2
Semi-trivial steady states of the system (1)–(4).

	"Biological control-free" steady state	Sufficient condition for the existence of the steady state
Without crop	$\left(0, \frac{A}{d_P}, 0, 0\right)$	No
With crop	$\left(C^*, P_H^* = \frac{A}{d_P - \frac{acC^*}{b+C^*}}, 0, 0\right)$	Condition I
	"Unavailable biological control" steady state	
Without crop	$\left(0, \frac{d_W(d_P+\epsilon)}{e\beta}, \frac{Ae\beta - d_W d_P(d_P+\epsilon)}{e\beta(d_P+\epsilon)}, \frac{Ae\beta - d_W d_P(d_P+\epsilon)}{d_W\beta(d_P+\epsilon)}\right)$	Condition II

Condition I: Harvest rate of the crop $h > r - \frac{Aa}{bd_P}$;

Condition II: Immigration rate of susceptible pests $A \geqslant \frac{d_P d_W(d_P+\epsilon)}{e\beta}$;

$C^* = \frac{(ac-d_P)(r-h)+bd_P\kappa - \sqrt{((ac-d_P)(r-h)+bd_P\kappa)^2 + 4(ac-d_P)\kappa(Aa-bd_P(r-h))}}{2(ac-d_P)\kappa}$.

and the immigration rate of susceptible pests A satisfies

$$A > A^*,$$

then the system has two positive steady states $(C_i^*, P_{H_i}^*, P_{I_i}^*, W_i^*)$, $i \in \{1,2\}$, where

$$P_{H_i}^* = \frac{d_W(d_P+\epsilon)}{e\beta},$$
$$P_{I_i}^* = \frac{bce\beta\kappa C_i^* + Ae\beta - bce(r-h)\beta + d_W(d_P+\epsilon)(ac-d_P)}{e\beta(d_P+\epsilon)},$$
$$W_i^* = \frac{bce\beta\kappa C_i^* + Ae\beta - bce(r-h)\beta + d_W(d_P+\epsilon)(ac-d_P)}{d_W\beta(d_P+\epsilon)}.$$

It is seen that

$$C_1^* > C_2^*, \quad P_{H_1}^* = P_{H_2}^*, \quad P_{I_1}^* = P_{I_2}^*, \quad W_1^* > W_2^*.$$

Case II : If the harvest rate of the crop h satisfies

$$h \in \left(\max\left\{0, r - \frac{ad_W(d_P+\epsilon)}{be\beta}\right\}, \min\left\{r\left(1+\frac{b}{K}\right) - 2\sqrt{\frac{\kappa a d_W(d_P+\epsilon)}{e\beta}}, r\left(1-\frac{b}{K}\right)\right\}\right)$$

and the immigration rate of susceptible pests A satisfies

$$A_* < A < A^*,$$

then the system has a unique positive steady state $(C_1^*, P_{H_1}^*, P_{I_1}^*, W_1^*)$.

Case III : If the harvest rate of the crop h satisfies

$$0 < h < \min\left\{r - \frac{ad_W(d_P+\epsilon)}{be\beta}, r\left(1-\frac{b}{K}\right)\right\}$$

or

$$h \in \left(r\left(1-\frac{b}{K}\right), r - \frac{ad_W(d_P+\epsilon)}{be\beta}\right)$$

and the immigration rate of susceptible pests A satisfies

$$A > A_*,$$

then the system still has the unique positive steady state $(C_1^*, P_{H_1}^*, P_{I_1}^*, W_1^*)$.

The Jacobian matrix J of the Eqs. (1)–(4) at the stationary point $(C_i^*, P_{H_i}^*, P_{I_i}^*, W_i^*)$ $(i = 1,2)$ can be evaluated as follows:

$$J = \begin{pmatrix} \frac{C_i^*(r-h-b\kappa-2\kappa C_i^*)}{b+C_i^*} & -\frac{aC_i^*}{b+C_i^*} & 0 & 0 \\ \frac{abcP_{H_i}^*}{(b+C_i^*)^2} & -\frac{A}{P_{H_i}^*} & 0 & -\beta P_{H_i}^* \\ 0 & \beta W_i^* & -(d_P+\epsilon) & \beta P_{H_i}^* \\ 0 & 0 & e & -d_W \end{pmatrix}.$$

In this regard, it is known that if all eigenvalues of J corresponding to a stationary point have strictly negative real parts, then the stationary point is stable, while if there is an eigenvalue with positive real part, then the stationary point is unstable.

Since the immigration rate of susceptible pests, A, and the crop harvest rate, h, are easy to be monitored and recorded by farmers, we fix all other parameters except A and h, and illustrate the fact that the immigration rate and the harvest rate have a significant impact on the dynamics of the solutions of (1)–(4). We use the following parameter values: $e = 2 \times 10^6$ polyhedron m^2 pest^{-1} ml^{-1} day^{-1}, $\beta = 3.5 \times 10^{-10}$ ml polyhedron^{-1} day^{-1}, together with the other values given in Table 1.

It is first noted that, from the above-mentioned **Case I**, the Eqs. (1)–(4) always have two positive equilibria if the harvest rate $h \in (0.27, 0.31)$ and the immigration rate of susceptible pests A satisfies $A > A^*$, in which the minimal value of A^* is approximately equal to 2 pest m^{-2} day^{-1}. It also follows from a stability analysis and from numerical simulations that the "larger crop production" equilibrium $(C_1^*, P_{H_1}^*, P_{I_1}^*, W_1^*)$ is asymptotically stable, while the "lower crop production" equilibrium $(C_2^*, P_{H_2}^*, P_{I_2}^*, W_2^*)$ is unstable. This indicates that the crop population escapes the low-density regulatory process since an exterior force such as pest species immigration or disease propagation acts to stabilize or increase the size of the infected pest population. From a theoretical viewpoint, in this case the "without crop" equilibrium is certainly unstable, while the stability of the other two semitrivial equilibria does not appear to be clear-cut, depending upon the concrete values chosen for the parameters of the model.

Secondly, in **Case II**, the Eqs. (1)–(4) have a unique positive equilibrium if the harvest rate still belongs to (0.27,0.31) and the immigration rate of susceptible pests A belongs to the interval (A_*, A^*), in which the maximal value of A^* is approximately equal to 2 pest m^{-2} day^{-1}. Since, biologically speaking, pest outbreaks are often caused by large numbers of immigrant pests, rather than very low numbers, this situation seldom occurs in the real world.

Thirdly, when considering the comparatively low harvest rate $h(< 0.27)$ and any immigration rate of susceptible pests that satisfies the conditions in **Case III**, the Eqs. (1)–(4) have a unique positive equilibrium, which is asymptotically stable, as confirmed by numerical simulations. It is to be noted that the situation of Case III is not desirable, since only a lower harvest rate h can be allowed, even with a large allowable interval for the pest immigration rate A, and the farmers should pursue the highest possible harvest rate, for the highest possible profit.

Recalling the statement on the steady state of the crop population together with its biological significance for biological pest control regimes, it is then seen that larger POBs production, e, or higher virus transmission β lead to an improved crop yield even under the assumption of a relatively high harvest rate, as illustrated by Fig. 2.

2.4. Within-pest virus dynamics: analytic findings

From a biological viewpoint and a cost-benefit analysis, in this pest control regime the emphasis is on control, not on eradication and the growers intend to release a "suitable" dose of pathogenic viruses, as shown in Fig. 3.

Using [67], we can get the dimensionless "virus reproductive ratio"

$$R_0 = \frac{C_{\max}\gamma(\alpha N - k_{va})(\mu_{\max} - d_C)}{\mu_{\max}(F - V_0)}.$$

As showcased in Fig. 3, if $R_0 < 1$, then the within-pest viral infection can not establish itself and the within-pest virus-free equilibrium

$$\left(\frac{C_{\max}(\mu_{\max} - d_C)}{\mu_{\max}}, 0, 0\right)$$

is globally asymptotically stable. However, if $R_0 > 1$, then the infection evolves in such a manner that the amounts of uninfected cells, infected cells and budded viruses tend to a unique globally asymptotically stable positive equilibrium

$$\left(C_U^* = \frac{(F - V_0)}{\gamma(\alpha N - k_{va})}, C_I^* = \frac{(F - V_0)(R_0 - 1)}{\gamma(\alpha N - k_{va})\left(1 + \frac{d_V R_0}{\mu_{\max} - d_C}\right)}, V^* = \frac{d_V(R_0 - 1)}{\gamma\left(1 + \frac{d_V R_0}{\mu_{\max} - d_C}\right)}\right). \tag{8}$$

This result can be used to estimate the steady level of the virus titre in some vital tissues such as invertebrate cuticle, body fat and midgut. In this regard, increasing the level of the virus titre will lead to the destruction of tissues which will eventually trigger the death of the pest individual and the spread of POBs containing viral particles.

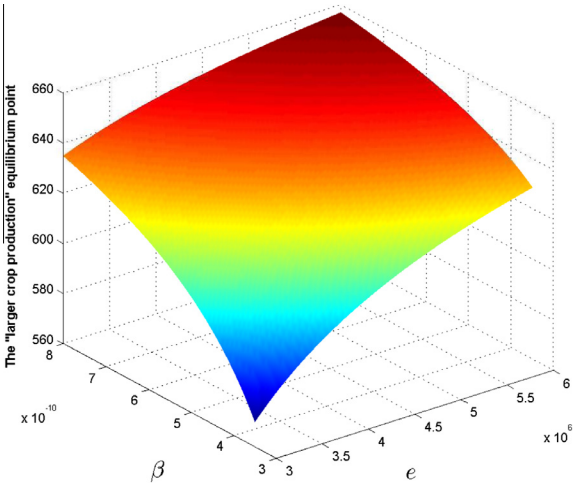

Fig. 2. The dependence of the crop yield at the "larger crop production" equilibrium upon the parameters e and β. Here, $r = 0.45$, $K = 900$, $a = 0.1$, $b = 100$, $c = 0.5$, $d_P = 0.01$, $d_W = 0.6$, $\epsilon = 0.6$, $h = 0.1$ and $A = 2$.

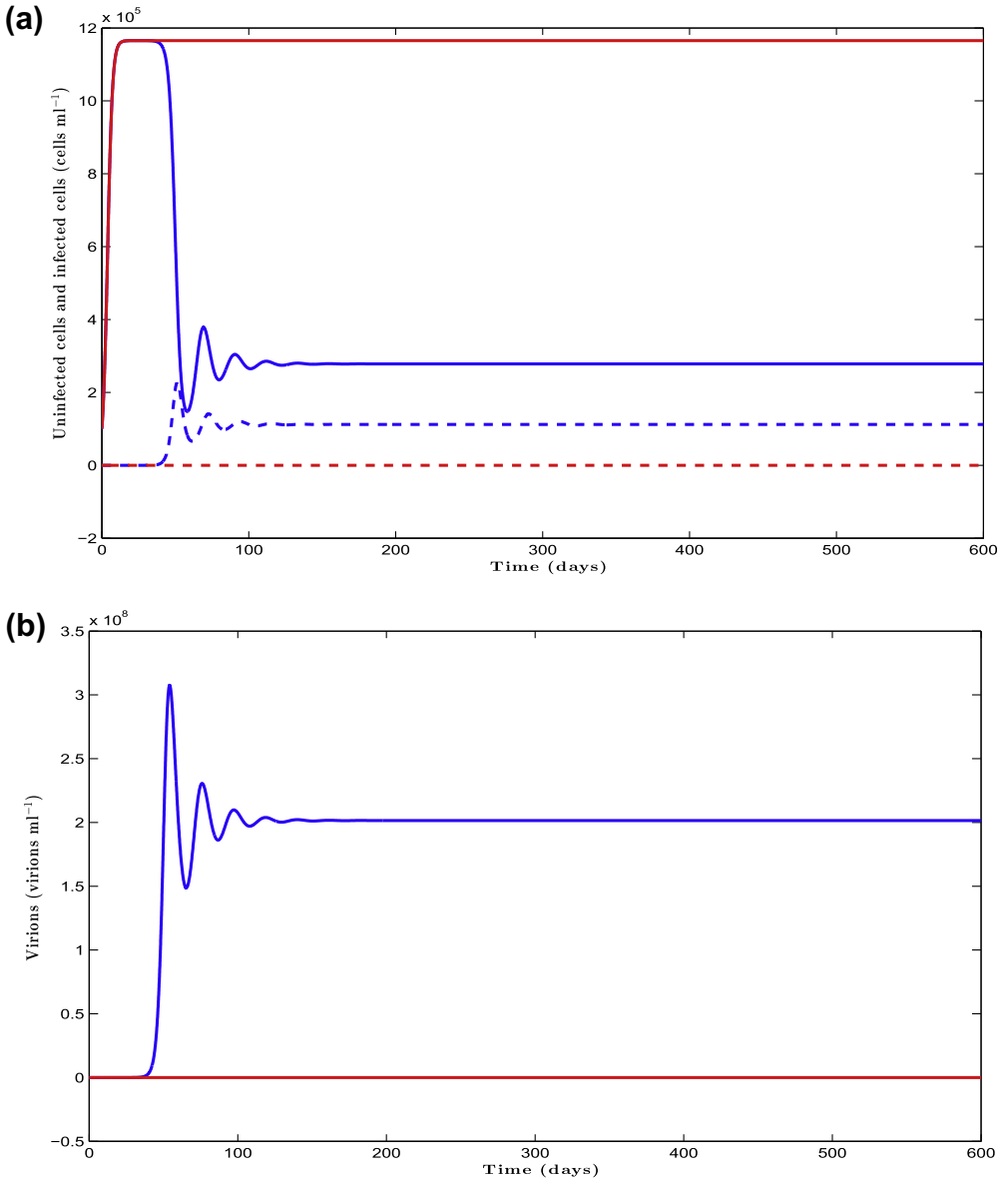

Fig. 3. Model simulations of cell infection and virus yield. (a) Blue curve and blue dashed curve represent uninfected and infected cells, respectively, for $R_0 \approx 4.2 > 1$ ($\gamma = 2 \times 10^{-9}$ ml virus^{-1} day^{-1}, $d_V = 1$ day^{-1}, $k_{va} = 0.8$ viruses cell^{-1}, $V_0 = 0.1$ day^{-1}); Red curve and red dashed curve represent uninfected and infected cells, respectively, with $R_0 \approx 0.42 < 1$ ($\gamma = 2 \times 10^{-10}$ ml virus^{-1} day^{-1}, $d_V = 1$ day^{-1}, $k_{va} = 0.8$ viruses cell^{-1}, $V_0 = 0.1$ day^{-1}). (b) Blue curve and red curve represent the viruses corresponding to $R_0 \approx 4.2$ and the viruses corresponding to $R_0 \approx 0.42$, respectively. Here $(C_U(0), C_I(0), V(0)) = (10^5, 0, 0.5)$. (For interpretation of the references to color in this figure legend, the reader is referred to the web version of this article.)

2.5. The relationship between within-pest virus dynamics and crop-pest-POBs dynamics

Here, we couple the within-pest virus dynamics with the dynamics of the crop-pest-POBs system by building some relationships between several parameters of these systems. Since the infected fluid, containing a large amount of POBs, further spreads infection when healthy larvae came in contact with the fluid, the probability of releasing and acquiring POBs increases with budded virus titre [68]. We then model this relationship as

$$e(m) = \theta_1 \frac{\phi_1 V^*}{1 + \phi_1 V^*} \tag{9}$$

and

$$\beta(m) = \theta_2 \frac{\phi_2 V^*}{1 + \phi_2 V^*}, \tag{10}$$

where $\theta_i (i = 1, 2)$ are shape parameters and $\phi_i (i = 1, 2)$ are rescaling parameters. Pests with a high ratio of infected to healthy cells in the vital organs will have larger mortality rates as a result of the disease. Hence, from the Eq. (6), the disease-related mortality rate, ϵ, increases with the ratio $\frac{\gamma V^*}{d_V(m)}$. Due to a lack of the information about this aspect, we then take for the sake of convenience a simple nonlinear relationship as follows

$$\epsilon(m) = \theta_3 \left(\frac{\gamma V^*}{d_V(m)} \right)^{\lambda}, \tag{11}$$

in which θ_3 is a rescaling constant and λ describes the severity or remission of symptoms.

3. The variable trait and the defence mechanisms

3.1. The variable trait

As mentioned in the previous sections, we restrict our attention to the multiplicity of infection (MOI). In what follows, we shall vary its value in order to modify the infectivity of the viruses in the host organs and then model the development of defence mechanisms. Here, according to the available data [69], we use the cubic curve fitter to find an approximating curve of the function $d_V(m)$ (see Fig. 4(a))

$$d_V(m) = -0.00091886m^3 + 0.029521m^2 - 0.23353m + 1.4123. \tag{12}$$

As for another important coefficient k_{va}, here is where the tricky part lies. If the cells are infected at a MOI of one, does that mean that each cell in the organ receives one virus? The answer is No. But we still believe that the rate of viral attachment increases with increasing MOI, and at sufficiently high MOI, target cells should be infected by several viruses. We then take a simple case of an exponential law relationship, (see Fig. 4(b)), due again to lack of information about this mechanism

$$k_{va}(m) = k_{va_{\max}}(1 - e^{-m}), \tag{13}$$

in which $k_{va_{\max}}$ is the maximal attachment rate. In Fig. 4, we present the dependence of d_V, k_{va}, $\frac{C_I^*}{C_U^*}$ and V^* on the value of MOI by solving the Eqs. (5)–(7) with (12) and (13). As shown in Fig. 4(c) and (d), the ratio of the equilibrium concentration of infected cells to the equilibrium concentration of uninfected cells, $\frac{C_I^*}{C_U^*}$ evolves in four phases including two inflection points, an initial rapid fall, a subsequent slight rise, a subsequent rapid fall and a final rapid rise, while V^* evolves in three dominant phases including an inflection point, an initial rapid fall, a subsequent slight rise and a final slight fall. In fact, at a low MOI the value of d_V has a rapid fall and the value of k_{va} has a rapid rise, which directly leads to an initial rapid fall of V^* because of

$$V^* = \frac{(R_0 - 1)}{\gamma\left(\frac{1}{d_V} + \frac{R_0}{\mu_{\max} - d_C}\right)}$$

and

$$R_0 \propto 1 - \frac{k_{va}}{\alpha N}.$$

However, at a slightly high or high MOI the value of k_{va} remains almost unchanged (see Fig. 4(b)). Furthermore, for the steady states, from (8),

$$\frac{C_I^*}{C_U^*} \propto \frac{1}{1 + \xi d_V},$$

in which

$$\xi \approx \frac{C_{\max}\gamma(\alpha N - k_{va_{\max}})}{\mu_{\max}(F - V_0)}.$$

3.2. The defence mechanisms

In this paper, analytical models of resistance mechanisms are used in order to take advantage of having well-worked-out mathematical methods for exploring the dynamics of the system, which yield results that are easy to understand and interpret [70]. On the basis of the literature survey performed in the Introduction, we model the variation of certain specific and structural defence mechanisms by introducing several resistance parameters.

3.2.1. Peritrophic membrane defence mechanism

Peritrophic membrane resistance relates to a reduction in the dilution rate of viruses, V_0, which are swallowed and then absorbed into the hemolymph. Introducing the resistance parameter, we write:

$$V_0 = (1 - \tau_{V_0})\tilde{V}_0, \tag{14}$$

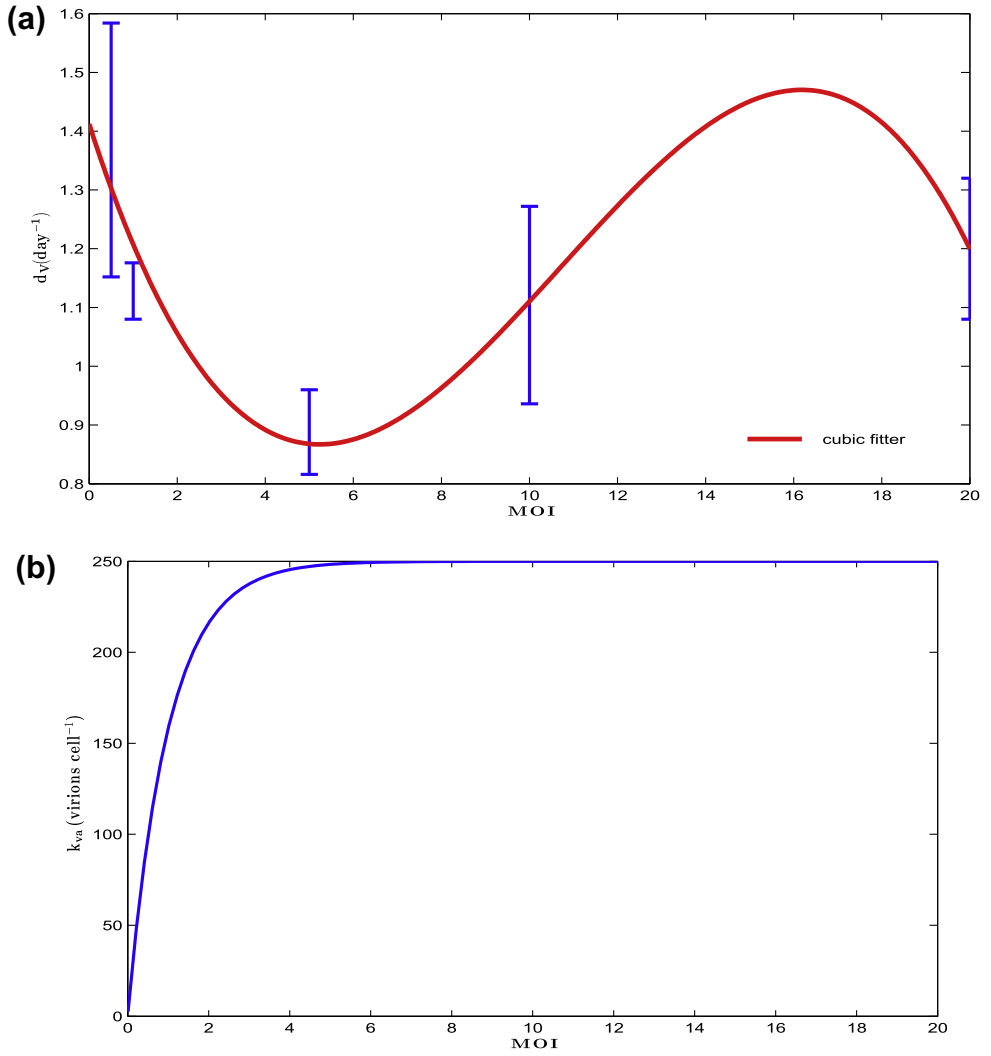

Fig. 4. (a) The relationship between the MOI ($m \in [0.01, 20]$) and d_V (day^{-1}). Here, we use the following data ($m = 0.5$, $d_V = (0.057 \pm 0.009) * 24$), ($m = 1, d_V = (0.047 \pm 0.002) * 24$), ($m = 5, d_V = (0.037 \pm 0.003) * 24$), ($m = 10, d_V = (0.046 \pm 0.007) * 24$), ($m = 20, d_V = (0.035 \pm 0.005) * 24$) given in [69]; (b) The relationship between the MOI ($m \in [0.01, 20]$) and k_{va} (day^{-1}) viruses cell^{-1}; (c) The relationship between the MOI ($m \in [0.01, 20]$) and the steady states of the Eqs. (5)–(7). The ratio of the steady state of infected cells to the steady state of uninfected cells, which is numerically equivalent to $\frac{\gamma V^*}{d_V}$, as a function of the MOI without the resistance mechanisms (blue solid curve) and, respectively, with the resistance mechanisms (blue dashed curve). The arrow indicates the effect of the peritrophic membrane resistance and the phagocytosis resistance; (d) The steady states of viruses as a function of the MOI without the resistance mechanisms (red solid curve) and, respectively, with the resistance mechanisms (red dashed curve). The arrow indicates the effect of the peritrophic membrane resistance and the phagocytosis resistance. Here, we choose $k_{va_{\max}} = 250$ viruses cell^{-1}, $\gamma = \tilde{\gamma} = 2 \times 10^{-9}$ ml virus^{-1} day^{-1}, $V_0 = \tilde{V}_0 = 0.1$, $\tau_\gamma = 0.2$, $\tau_{V_0} = 0.5$, the other parameters being given in Table 1. (For interpretation of the references to color in this figure legend, the reader is referred to the web version of this article.)

where τ_{V_0} is a parameter with values between 0 and 1. It follows from (8) that for values of the resistance parameter τ_{V_0} close to the unity, the virus concentration decreases (Fig. 4(c) and (d)).

3.2.2. Phagocytosis defence mechanism

Phagocytosis resistance relates to a reduction of the virus infection rate, γ, in the vital organs. We write

$$\gamma = (1 - \tau_\gamma)\tilde{\gamma}, \tag{15}$$

where τ_γ is a parameter with values between 0 and 1. Again, for values of the resistance parameter τ_γ close to the unity, the virus concentration decreases (Fig. 4(c) and (d)).

3.2.3. Unknown virus titre-reducing defence mechanism

Since biochemical events lead to characteristic cell changes and death, we model the baculovirus IAP by reducing the virus titre. Also, quantitative information about the other mechanisms by which the virus titre is reduced is largely unavail-

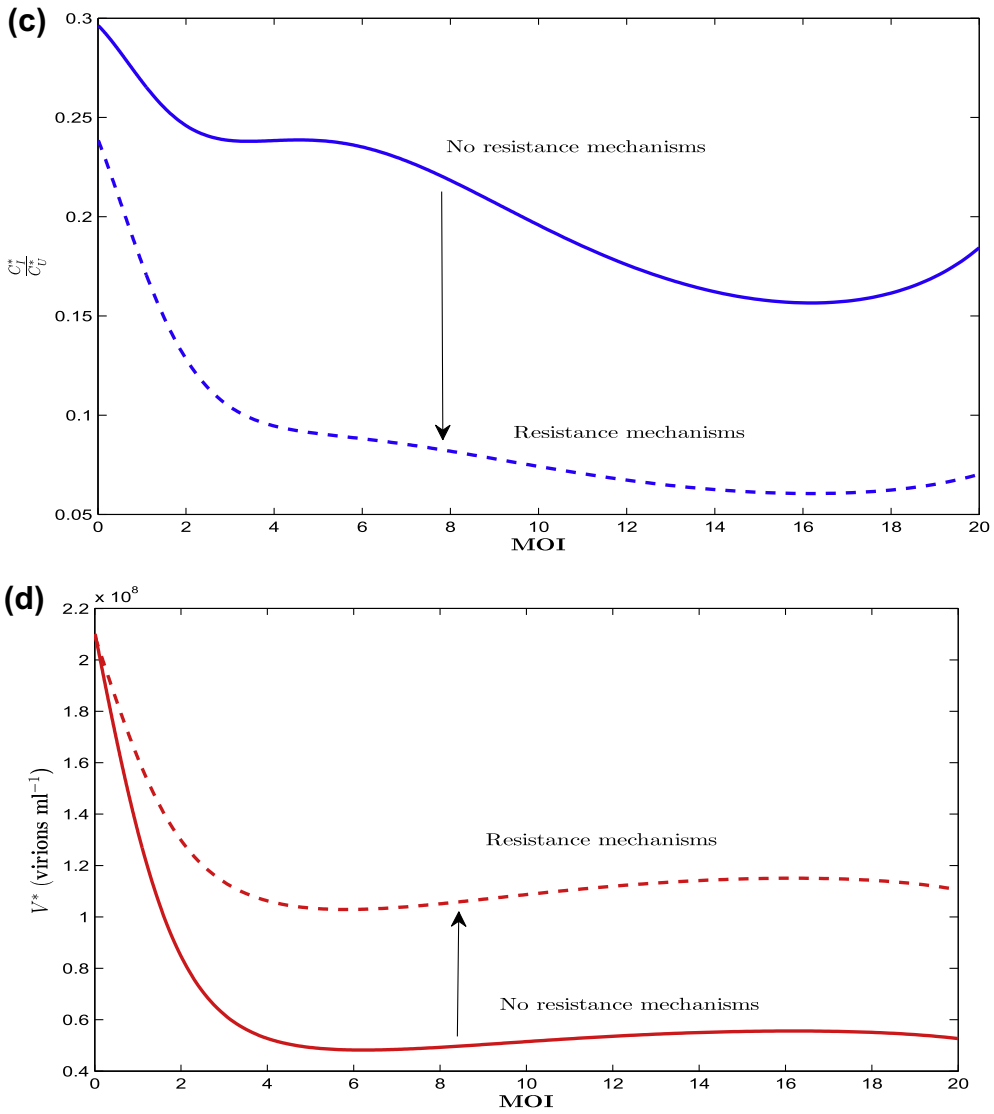

Fig. 4 (*continued*)

able. We then model this type of resistance by assuming that the steady-state virus concentration, V^*, is multiplied by a factor $1-\tau_V$, in which τ_V is a parameter with values between 0 and 1. When the value of this resistance parameter τ_V is close to unity, the virus is effectively removed, which indicates that this increase keeps the healthy pests from contracting the disease (Fig. 5(a) and (b)).

3.2.4. Cuticle defence mechanism

Cuticle resistance relates, in the crop-pest-POBs model, to a reduction of the production rate of the POBs, e, by a factor $1-\tau_e$. We then write:

$$e = (1-\tau_e)\tilde{e}, \tag{16}$$

in which τ_e is a parameter with values between 0 and 1. The equilibrium density of healthy pests increases with increasing resistance (Fig. 5(c)). The biomass of the soybean crop population at equilibrium decreases with increasing resistance (Fig. 5(d)).

3.2.5. Contact-reducing defence mechanism

Contact-reducing resistance relates to a reduction of the contact rate, β, in the crop-pest-POBs model. We write:

$$\beta = (1-\tau_\beta)\tilde{\beta}. \tag{17}$$

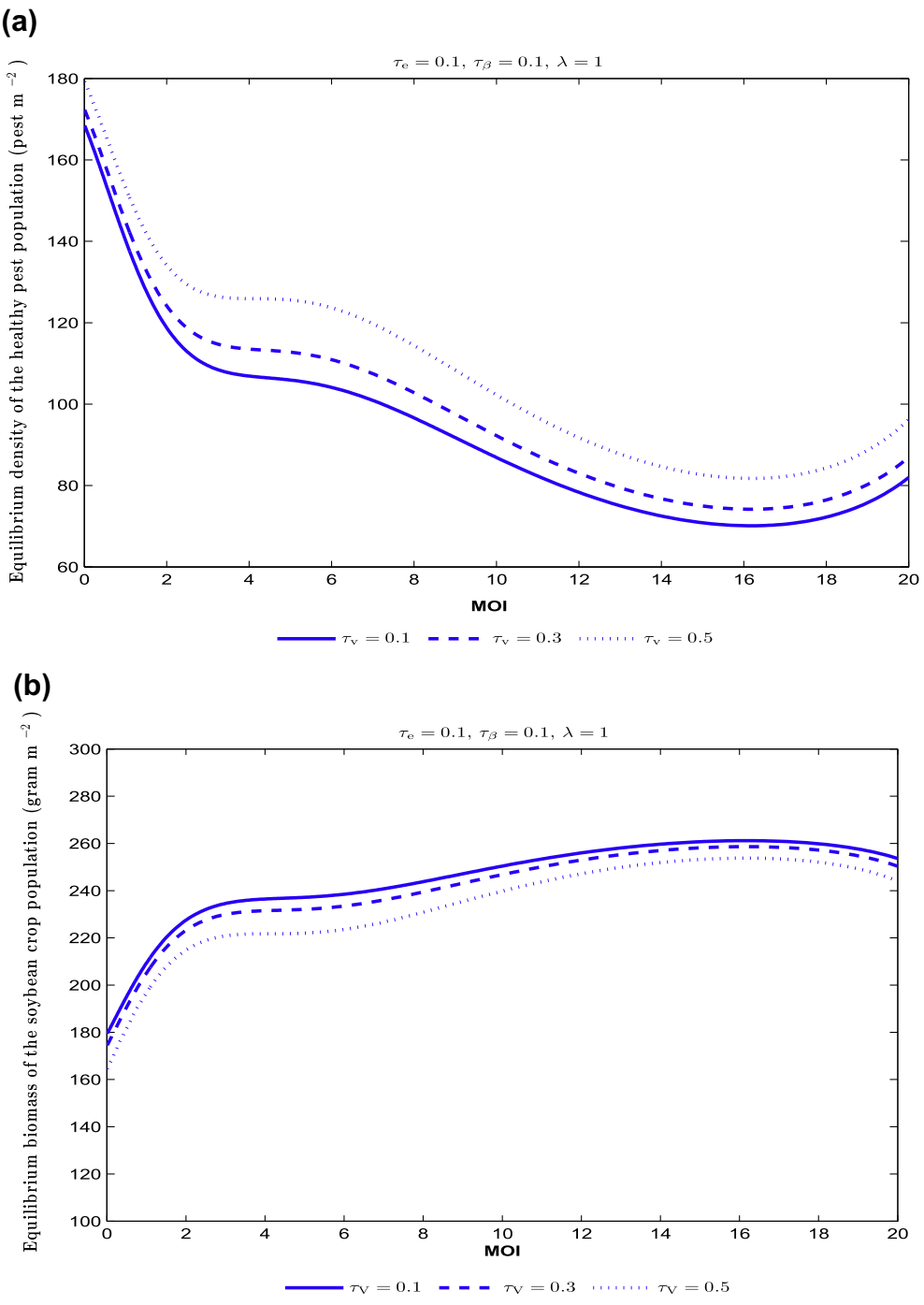

Fig. 5. (a) The relationship between different values of MOI and the steady states of the healthy pest population coupled with unknown virus titre-reducing resistance regimes ($\tau_V = 0.1, 0.3, 0.5$). (b) The relationship between different values of MOI and the steady states of the crop population coupled with unknown virus titre-reducing resistance regimes ($\tau_V = 0.1, 0.3, 0.5$). (c) The relationship between different values of MOI and the steady states of the healthy pest population coupled with cuticle resistance regimes ($\tau_e = 0.1,\ 0.15,\ 0.2$). (d) The relationship between different values of MOI and the steady states of the crop population coupled with cuticle resistance regimes ($\tau_e = 0.1, 0.15, 0.2$). (e) The relationship between different values of MOI and the steady states of the healthy pest population coupled with contact-reducing resistance regimes ($\tau_\beta = 0.05, 0.1, 0.2$). (f) The relationship between different values of MOI and the steady states of the crop population coupled with contact-reducing resistance regimes ($\tau_\beta = 0.05, 0.1, 0.2$). Here, we choose $h = 0.3$ day^{-1}, $A = 50$ pest m^{-2} day^{-1}, $k_{v\alpha_{\max}} = 250$ viruses cell^{-1}, $\gamma = \bar{\gamma} = 2 \times 10^{-9}$ ml virus^{-1} day^{-1}, $V_0 = \bar{V}_0 = 0.1$, $\tau_\gamma = 0.2$, $\tau_{V_0} = 0.5$, $\phi_1 = 2 \times 10^{-7}$, $\phi_2 = 10^{-7}$, $\theta_1 = 5 \times 10^6$, $\theta_2 = 5 \times 10^{-10}$, $\theta_3 = 2$, the other parameters being given in Table 1.

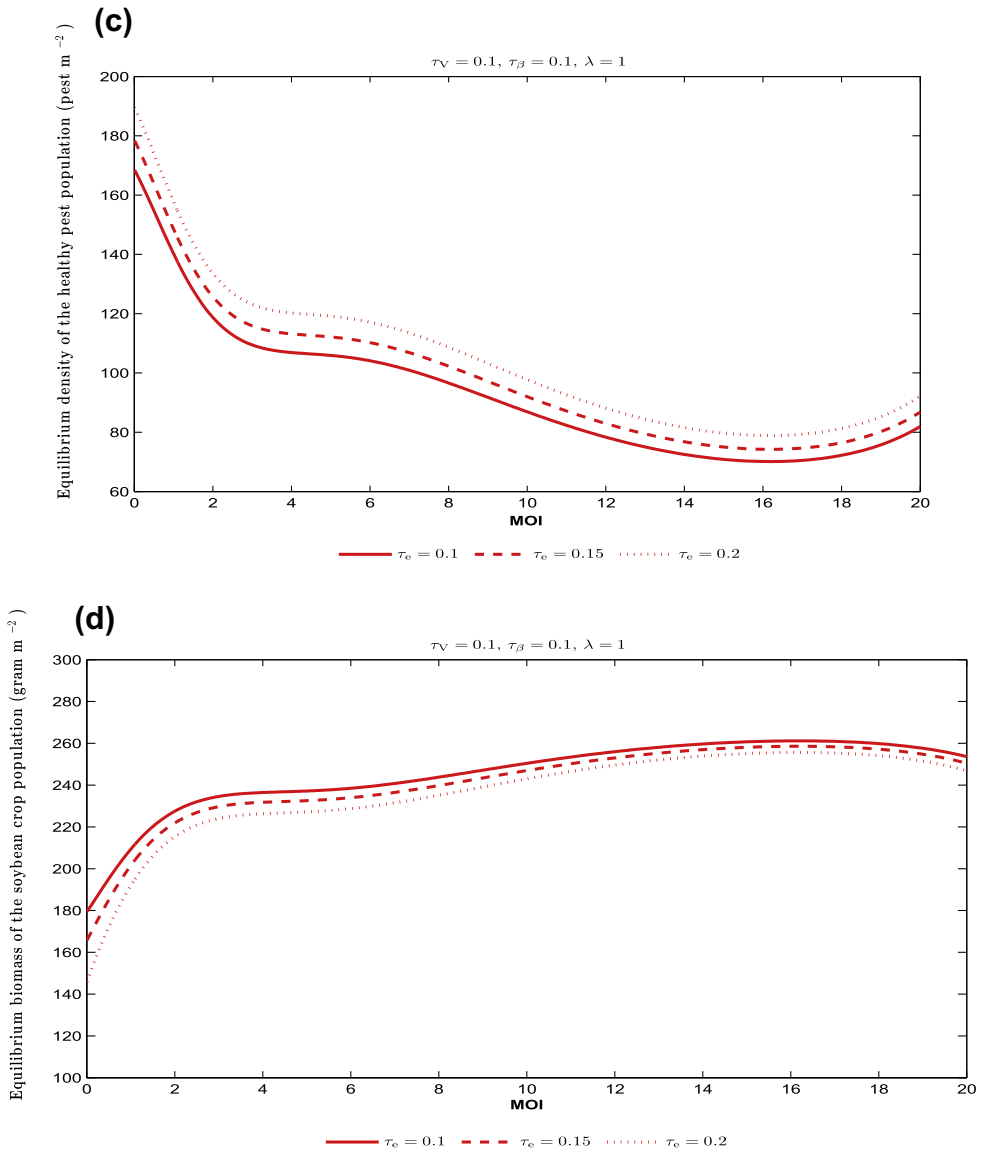

Fig. 5 (*continued*)

in which τ_β is a parameter with values between 0 and 1. The results for the contact-reducing resistance differs only in minor quantitative details from those of the cuticle resistance shown (Fig. 5(e) and (f)).

4. Dynamics influenced by resistance mechanisms

Assume that the resident virus population has a resident trait, the multiplicity of infection m_{res}. According to the Eq. (8) and to the above-mentioned considerations on the resistance mechanisms, the steady state density of the resident viruses is then given by

$$V^*_{res} = (1-\tau_V)V^*\left(\mu_{\max}, C_{\max}, d_C, (1-\tau_\gamma)\tilde{\gamma}, d_V(m_{res}), (1-\tau_{V_0})\tilde{V}_0, F, k_{va}(m_{res}), \alpha, N\right), \tag{18}$$

which implies that the ratio of the steady state densities of infected to healthy cells is given by

$$\frac{C^*_{I_{res}}}{C^*_{U_{res}}} = \frac{(1-\tau_\gamma)\tilde{\gamma}V^*_{res}}{d_V(m_{res})}, \tag{19}$$

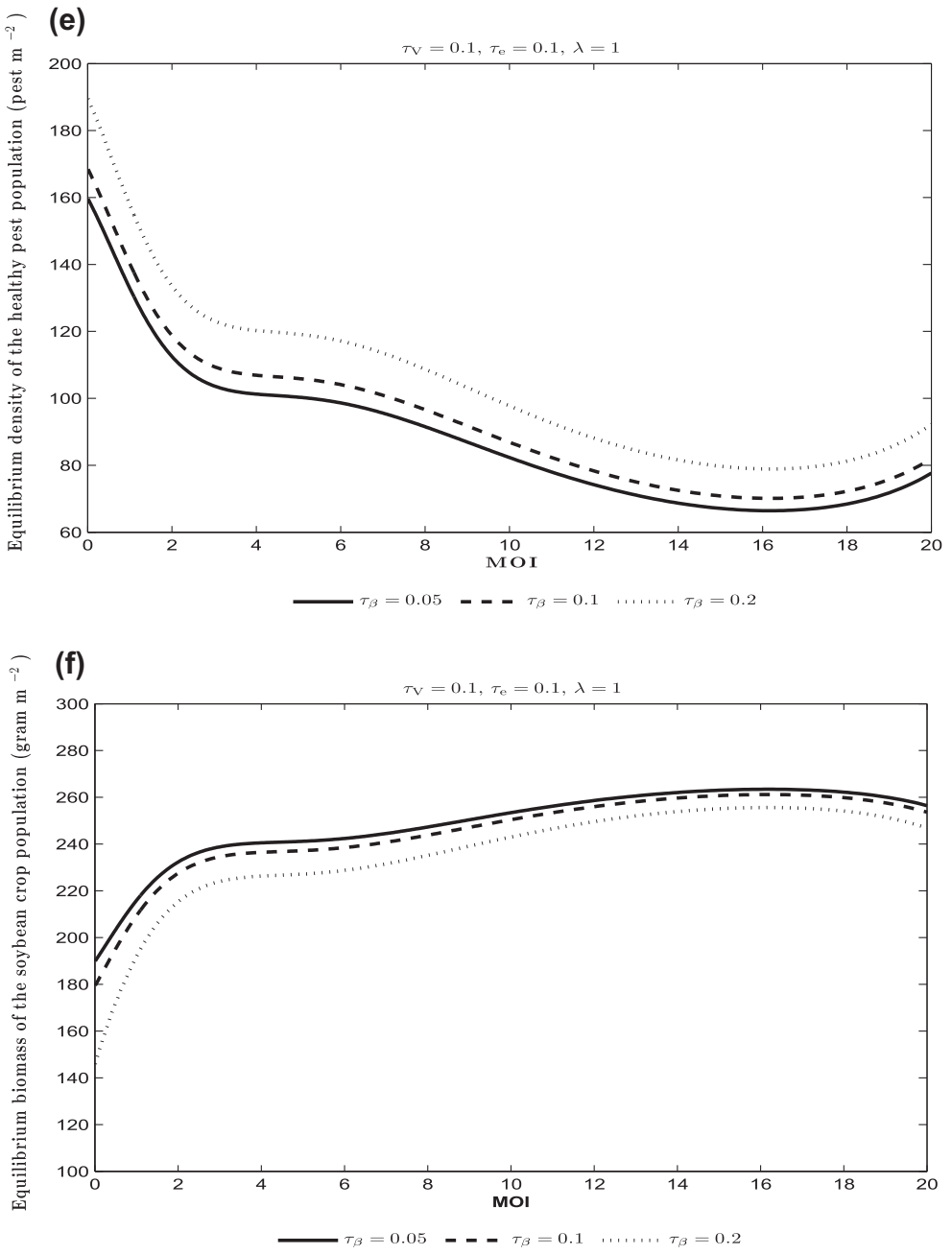

Fig. 5 (*continued*)

From (9)–(11), for the analysis of the dynamics of the healthy pest population and of the crop population, we use the following parameters coupled with the resistance regimes in the pest-crop model

$$\begin{aligned} e_{res} &= e(m_{res}) = (1-\tau_e)\theta_1 \frac{\phi_1 V^*_{res}}{1+\phi_1 V^*_{res}}, \\ \beta_{res} &= \beta(m_{res}) = (1-\tau_\beta)\theta_2 \frac{\phi_2 V^*_{res}}{1+\phi_2 V^*_{res}}, \\ \epsilon_{res} &= \epsilon(m_{res}) = \theta_3 \left(\frac{\tilde{R}_0(m_{res})-1}{1+\frac{d_V(m_{res})\tilde{R}_0(m_{res})}{\mu_{\max}-d_C}} \right)^{\lambda}, \end{aligned} \tag{20}$$

in which

$$\tilde{R}_0(m) = \frac{C_{\max}(1-\tau_\gamma)\tilde{\gamma}(\alpha N - k_{va}(m_{res}))(\mu_{\max} - d_C)}{\mu_{\max}(F-(1-\tau_{V_0})\tilde{V}_0)}.$$

As shown in Fig. 6, the equilibrium density of healthy pests dramatically decreases with slightly increasing symptom severity (see Fig. 6(a)), which directly increases the equilibrium biomass of the soybean crop population (see Fig. 6(b)). For simplicity, we assume that, before the arrival of a mutant, the density of the resident healthy pest population with trait m_{res} at equilibrium is given by

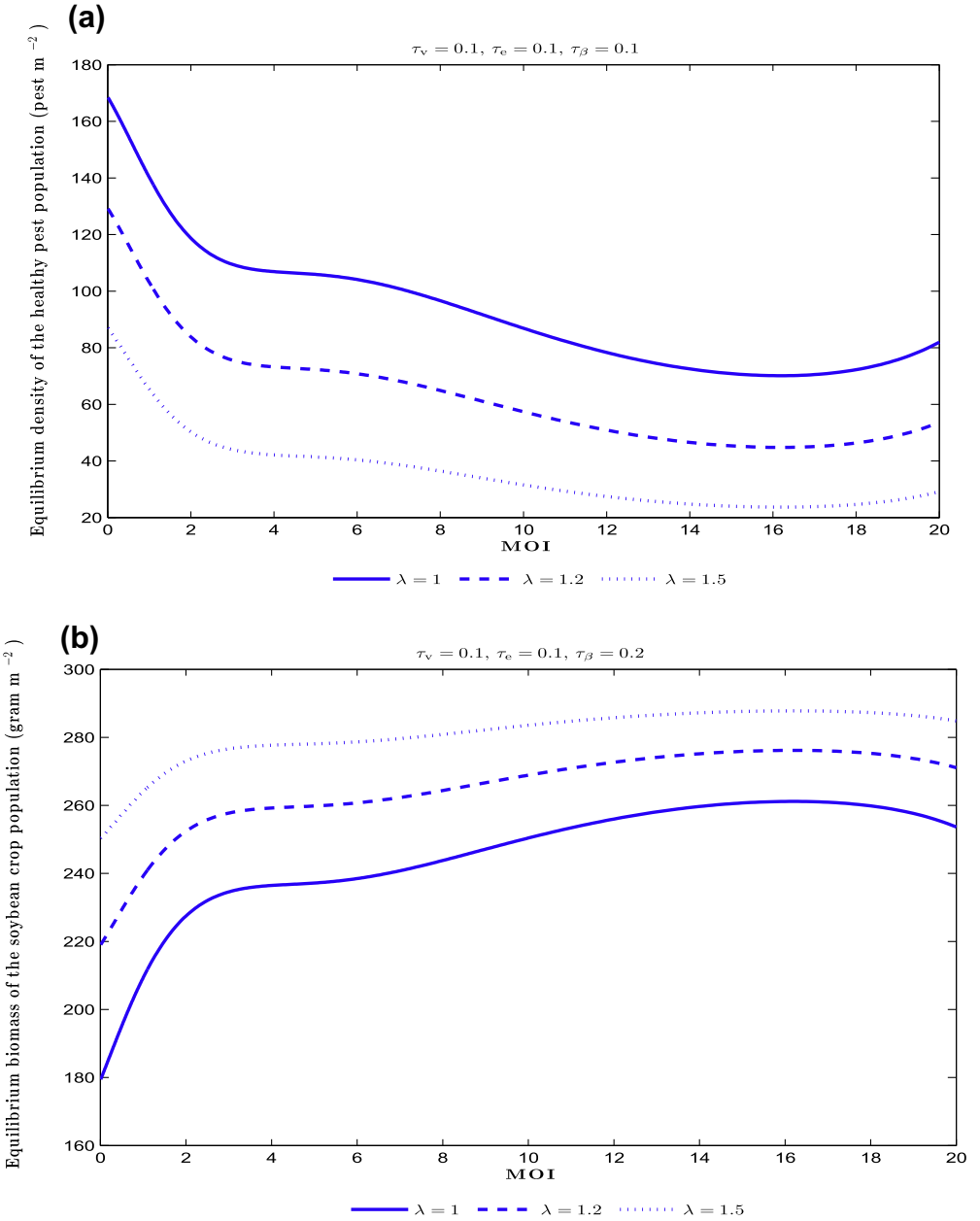

Fig. 6. (a) The relationship between different values of MOI and the steady states of the healthy pest population coupled with different values of λ that increase or decrease the disease-related mortality rate of infected pests ($\lambda = 1, 1.2, 1.5$). (b) The relationship between different values of MOI and the steady states of the crop population coupled with different values of λ that increase or decrease the disease-related mortality rate of infected pests ($\lambda = 1, 1.2, 1.5$). Here, we choose $h = 0.3$ day^{-1}, $A = 50$ pest m^{-2} day^{-1}, $k_{va_{\max}} = 250$ viruses cell^{-1}, $\gamma = \tilde{\gamma} = 2\times10^{-9}$ ml virus^{-1} day^{-1}, $V_0 = \tilde{V}_0 = 0.1$, $\tau_\gamma = 0.1$, $\tau_{V_0} = 0.5$, $\phi_1 = 2\times10^{-7}$, $\phi_2 = 10^{-7}$, $\theta_1 = 5\times10^6$, $\theta_2 = 5\times10^{-10}$, $\theta_3 = 2$, the other parameters being given in Table 1.

$$P^*_{H_{res}} = \frac{d_W(d_P + \epsilon_{res})}{e_{res}\beta_{res}}.$$

Assume that the mutant has trait m_{mut} such that $\tilde{R}_0(m_{mut}) > 1$. The lifetime reproductive success (LRS) of the mutant in the resident pest population at equilibrium [71], understood as a measure of individual ability to reproduce and pass down distinctive genes over the period of a lifetime, is then given by

$$\Re_0(m_{mut}, m_{res}) = P^*_{H_{res}} \frac{e_{mut}\beta_{mut}}{d_W(d_P + \epsilon_{mut})}. \tag{21}$$

Here, e_{mut}, β_{mut} and ϵ_{mut} all depend on the steady state density of the mutant viruses which is determined by the "inherent" regimes including the resident host uninfected cells and infected cells at the demographic equilibrium states $C^*_{U_{res}}$ and $C^*_{I_{res}}$. Consequently, the resident-mutant dynamics is determined by the following generalization of (7)

$$\frac{dV_{mut}(t)}{dt} = d_V(m_{mut})N\alpha C^*_{I_{res}} - (F - V_0)V_{mut}(t) - k_{va}(m_{mut})\gamma C^*_{U_{res}}V_{mut}(t). \tag{22}$$

If $\Re_0(m_{mut}, m_{res}) < 1$, then the mutant can not establish the viral infection in the pest population. However, we are looking for a resident m_{res} such that any mutant can establish the pest viral infection under the resistance mechanisms, which means that $\Re_0(m_{mut}, m_{res}) > 1$ for all m_{mut} except for $m_{mut} = m_{res}$, where $\Re_0(m_{mut}, m_{res}) = 1$.

The evolution of a monomorphic population can be analyzed by a graphically pairwise plot, which is a graph of the value of the function of the LRS of the mutant in the resident pest population at equilibrium states including two variables, the resident trait and the mutant trait. Specifically, in such plots, each point represents a combination of considered mutant and resident trait values and gives the value of the $\Re_0$. Along the main diagonal of the pairwise plot we can exploit the relation $\Re_0(m, m) = 1$, which implies that, by definition, the density of infected pests accurately replenishes itself once the disease has reached its endemic equilibrium [71].

As shown in Fig. 7 (interpretable as an invasibility plot), for the resident healthy pest population with lower MOI, one observes that any mutant can establish the pest viral infection under the evolutionary resistance mechanisms because of $\Re_0(m_{mut}, m_{res}) > 1$. Even though there are a wide distribution of resistance mechanisms and some "qualified" mutations defined by the assumption that $\tilde{R}_0(m_{mut}) > 1$ in the culture, low MOI infection is the best strategy for the growers to expand or amplify virus stocks. However, from Fig. 7, the point A represents the worst strategy, in which for this resident trait approximating 16.2 no invader can establish the viral infection in the pest population. That is, the invader will die out

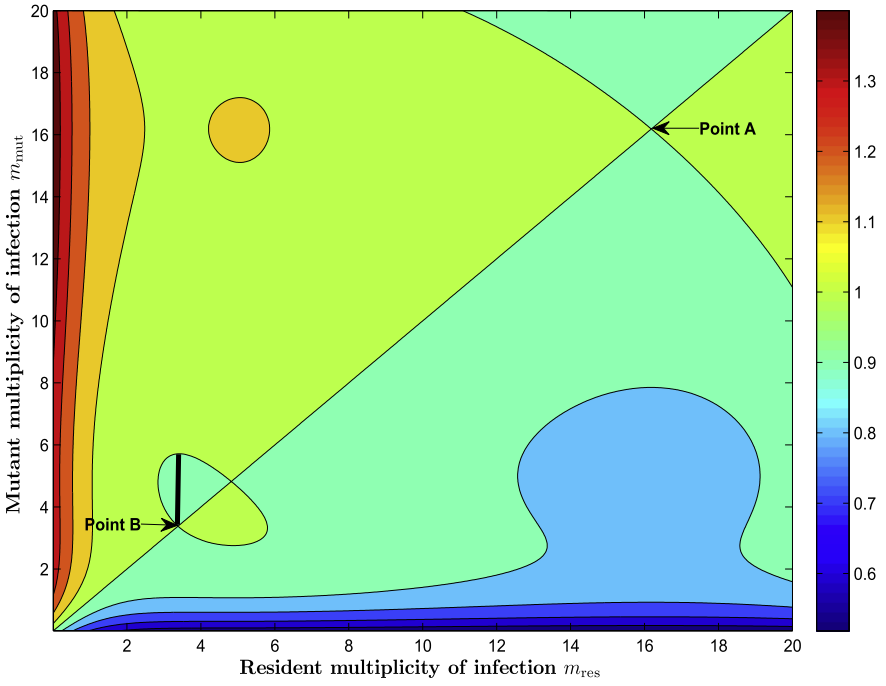

Fig. 7. The relationship between mutant trait value $m_{mut} \in [0.01, 20]$, resident trait value $m_{res} \in [0.01, 20]$ and the lifetime reproductive success of the mutant in the resident pest population at equilibrium states $\Re_0(m_{mut}, m_{res})$. Here, every color represents the $\Re_0$ value which can be read from the colorbar. Also, we choose $h = 0.3$ day^{-1}, $A = 50$ pest m^{-2} day^{-1}, $k_{va_{\max}} = 250$ viruses cell^{-1}, $\gamma = \bar{\gamma} = 2 \times 10^{-9}$ ml virus^{-1} day^{-1}, $V_0 = \bar{V}_0 = 0.1$, $\tau_\gamma = 0.1$, $\tau_{V_0} = 0.5$, $\tau_V = 0.1$, $\tau_\beta = 0.1$, $\phi_1 = 2 \times 10^{-7}$, $\phi_2 = 10^{-7}$, $\theta_1 = 5 \times 10^6$, $\theta_2 = 5 \times 10^{-10}$, $\theta_3 = 2$, the other parameters being given in Table 1.

and can not increase the endemicity of the disease even under circumstances including different resistance mechanisms. Also, a value of the MOI approximately equal to 3.4 (the point B) does not correspond to a good strategy because one still can observe a small area corresponding to some values of the mutant MOI (black bar) which signifies that not all mutants can establish the viral infection.

5. Discussion

Several studies have attempted to model pesticide resistance in a variety of ways, especially considering the traits of resistance to pesticides in arthropod pests. However, very few of them have considered modeling resistance by combining a within-pest model with a model accounting for various types of resistance in a population of hosts. This inspired us to propose a model coupling the within-pest virus dynamics with the crop-pest-POBs dynamics. The within-pest model is used to fine-tune the crop-pest-POBs dynamics by building relationships between several parameters of the crop-pest-POBs model and parameters of the within-pest model. Specifically, the relationship between the transmission rate β, the disease-related mortality ϵ and the proportionality constant e quantifying the POBs virus yield (characterizing the crop-pest-POBs model) and the multiplicity of infection (characterizing the within-pest model) is provided, which allows us to consider the influence of the MOI upon the dynamics of the disease in the pest population.

Also, in our settings two categories of virus responses to defence mechanisms can be considered: certain specific and structural defence mechanisms including a peritrophic membrane defence mechanism, a phagocytosis defence mechanism, a cuticle defence mechanism, a contact-reducing defence mechanism and an unknown virus titre-reducing defence mechanism. Considering only a few of the defence mechanisms (or considering them one by one) would lead to quantitative differences in the parameters which are subject to the numerical analysis, rather than in different qualitative properties. However, although qualitative aspects of the dynamics are not altered drastically, the differences in the magnitudes of ratio of the steady state of infected cells to the steady state of uninfected cells or the density of healthy pests at equilibrium, for instance, are enough to make a practical difference.

Besides the use of the model in distinguishing between different types of resistance, our work can also help developing hypotheses that can be tested experimentally:

(i) Expressing defence mechanisms through symptom reduction can eventually lead to the selection of within-pest virus strains which have a great impact on the lifetime reproductive success of the mutant which appears in the resident culture.
(ii) To establish the viral infection by invaders there is a threshold of the mutant trait, that is, $\tilde{R}_0(m_{mut}) > 1$.

The main feature of our work is that we proposed and investigated a coupled crop-pest-virus model which accounts for different defence regimes and established that low MOI infection is the best strategy for expanding or amplifying virus stocks and establishing the viral infection in the pest population, which directly increases the yield of the crop. Also, we can estimate the possible value of the resident trait m_{res} for which no mutant can establish the pest viral infection under the given defence responses. In this regard, we mainly focused on the lifetime reproductive success of the mutant in the resident pest population at equilibrium, not on the evolutionary dynamics of the mutant, which makes the perspective of our paper different from that of the majority of papers on evolutionary dynamics.

Until now, only a few studies were concerned with finding the parameters through which defence is expressed, and no adequate test of the hypotheses above is available. Although our model has a rather static (as opposed to adaptive) perspective upon these defence mechanisms, we have investigated five distinct types of resistance which are biologically valid, our model being then used to obtain, via numerical simulations, conclusions which are meaningful from a practical viewpoint. Our conclusions may then inspire other studies to gather and test experimental data, as well as to improve the mechanistical background of the defence mechanisms.

Acknowledgments

The work of H. Zhang was supported by the National Natural Science Foundation of China, Grant ID 11201187, the Scientific Research Foundation for the Returned Overseas Chinese Scholars and the China Scholarship Council. The work of P. Georgescu was supported by a Grant of the Romanian National Authority for Scientific Research, CNCS UEFISCDI, Project number PN-II-ID-PCE-2011-3-0563, Contract No. 343/5.10.2011. Moreover, the authors would like to thank the anonymous referees for their valuable comments.

References

[1] J.E. Jansma, H. van Keulen, J.C. Zadoks, Crop protection in the year 2000: a comparison of current policies towards agrochemical usage in four West European countries, Crop Prot. 12 (1993) (2000) 483–489.
[2] D.T. Briese, Resistance of insect species to microbial pathogens, in: E.N. Davidson (Ed.), Pathogenesis of Invertebrate Microbial Diseases, Allanheld Osmum, New Jersey, 1981, pp. 511–545.
[3] A.J. Cherry, C.J. Lomer, D. Djegui, F. Schulthess, Pathogen incidence and their potential as microbial control agents in IPM of maize stemborers in West Africa, Biocontrol 44 (a) (1999) 301–327.

[4] J.S. Cory, M.L. Halis, T. Williams, R.S. Hails, D. Goulson, B.M. Green, T.M. Carty, R.D. Possee, P.J. Cayley, D.H.L. Bishop, Field trial of a genetically improved baculovirus insecticide, Nature 370 (1994) 138–140.
[5] J.R. Fuxa, Ecology of insect nuclear polyhedrosis viruses, Agric. Ecosyst. Environ. 103 (2004) 27–43.
[6] P. Ferron, Pest control using the fungi Beauveria and Metarhizinm, in: H.D. Burgess (Ed.), Microbial Control in Pests and Plant Diseases, Academic Press, London, 1981, pp. 465–483.
[7] M.L. Luff, The potential of predators for pest control, Agric. Ecosys. Environ. 10 (1983) 159–181.
[8] Y. Zhang, B. Liu, L.S. Chen, Dynamical behavior of Volterra model with mutual interference concerning IPM, ESAIM Math. Mod. Numer. Anal. 38 (2004) 143–155.
[9] H. Zhang, L.S. Chen, J.J. Nieto, A delayed epidemic model with stage-structure and pulses for management strategy, Nonlinear. Anal.: Real World Appl. 9 (2008) 1714–1726.
[10] F. Moscardi, Assessment of the application of baculoviruses for control of lepidoptera, Ann. Rev. Entomol. 44 (1999) 257–289.
[11] A. Prasad, Y. Wadhwani, Pathogenic virus and insect tissues: an effective way of pest control, Current Sci. 91 (2006) 803–807.
[12] M.K. Singh, S.V.S. Raju, H.N. Singh, Laboratory bioassay of Bacillus thuriengiensis formulation against diamondback moth Plutella xylostella, Indian J. Entomol. 65 (2003) 86–93.
[13] N. Chejanovsky, E. Gershburg, The wild type Autographa californica nuclear polyhedrosis virus induced apoptosis of Spodoptera littoralis cells, Virology 209 (1995) 519–525.
[14] G.W. Blissard, Baculovirus–insect cell interactions, Cytotechnology 20 (1996) 73–93.
[15] G.W. Blissard, G.F. Rohrmann, Baculovirus diversity and molecular biology, Ann. Rev. Entomol. 35 (1990) 127–155.
[16] G.S. Dhaliwal, R. Arora, Principles of Insect Pest Management, Kalyani Publishers, New Delhi, 1998.
[17] B.E. Tabashnik, Modeling and evaluation of resistance management tactics, in: R.T. Roush, B.E. Tabashnik (Eds.), Pesticide Resistance in Arthropods, Chapman & Hall, New York, 1990, pp. 153–182.
[18] B.E. Tabashnik, B.A. Croft, Evolution of pesticide resistance in apple pests and their natural enemies, Entomophaga 30 (1985) 37–49.
[19] B.E. Tabashnik, Y.B. Liu, N. Finson, L. Masson, D.G. Heckel, One gene in diamondback moth confers resistance to four *Bacillus thuringiensis* toxins, Proc. Nat. Acad. Sci. USA 94 (1997) 1640–1644.
[20] M.A. Hoy, Myhts, models and mitigation of resistance to pesticides, Philos. Trans. R. Soc. Lond. B 353 (1998) 1787–1795.
[21] K. Narayanan, Insect defence: its impact on microbial control of insect pests, Current Sci. 86 (2004) 800–814.
[22] J.P. Gillespie, M.R. Kanost, T. Trenczeck, Biological mediators of insect immunity, Ann. Rev. Entomol. 42 (1997) 611–643.
[23] R.M. Anderson, R.M. May, Infectious disease and population cycles of forest insects, Science 210 (1980) 658–661.
[24] L.A. Falcon, Problem associated with the use of arthropod viruses in pest control, Ann. Rev. Entomol. 21 (1976) 305–324.
[25] F. Fenner, F.N. Ratcliffe, Myxomatosis, Cambridge University Press, Cambridge, 1965.
[26] V. Morell, Australian pest control by virus causes concern, Science 261 (1993) 683–684.
[27] Y. Tanada, in: P. DeBach (Ed.), Epizootiology of Insect Disease, Biological Control of Insect Pests and Weeds, Chapman and Hall, London, 1964 (pp. 548–578).
[28] N. Wade, Insect viruses: a new class of pesticides, Science 181 (1973) 925–928.
[29] A. Zeng, Q. Zhang, Z. Zhou, Y. Chen, R. Hu, J. Long, X. Li, C. Wu, Occurrence pattern of *Spodoptera litura* in Hunan and its prediction methods, 2011 6th IEEE Conference on Industrial Electronics and Applications, 2628–2632.
[30] R.M. Anderson, R.M. May, Regulation and stability of host–parasite population interactions. I. Regulatory processes, J. Anim. Ecol. 47 (1978) 219–247.
[31] R.M. Anderson, R.M. May, Infectious Diseases of Humans: Dynamics and Control, Oxford University Press, Oxford, 1991.
[32] R.M. Anderson, R.M. May, The population dynamics of microparasites and their invertebrate hosts, Philos. Trans. R. Soc. Lond. B 291 (1981) 451–524.
[33] R.M. Anderson, R.M. May, Population ecology of infectious disease agents, in: R.M. May (Ed.), Theoretical Ecology Principles and Applications, second ed., Sinauer Association, Sunderland, 1981, pp. 318–355.
[34] L. Berec, D. Maxin, Double impact of sterilizing pathogens: added value of increased life expectancy on pest control effectiveness, J. Math. Biol. 64 (2012) 1281–1311.
[35] C.J. Briggs, H.C.J. Godfray, The dynamics of insect–pathogen interactions in stage-structured populations, Am. Nat. 145 (1995) 855–887.
[36] G.C. Brown, Stability in an insect–pathogen model incorporating age-dependent immunity and seasonal host reproduction, Bull. Math. Biol. 46 (1981) 139–153.
[37] H.C.J. Godfray, C.J. Briggs, N.D. Barlow, M. O'Callaghan, T.R. Glare, T.A. Jackson, A model of insect–pathogen dynamics in which a pathogenic bacterium can also reproduce saprophytically, Philos. Trans. R. Soc. Lond. B 266 (1999) 233–240.
[38] T.K. Kar, A. Ghorai, S. Jana, Dynamics of pest and its predator model with disease in the pest and optimal use of pesticide, J. Theor. Biol. 310 (2012) 187–198.
[39] M. Moerbeek, F. Van den Bosch, Insect–pathogen dynamics: stage-specific and insect density dependence, Math. Biosci. 141 (1997) 115–148.
[40] B.R. Levin, R. Antia, E. Berliner, P. Bloland, S. Bonhoeffer, M. Cohen, T. DeRouin, P.I. Fields, H. Jafari, D. Jernigan, M. Lipsitch, J. McGowan, P. Mead, M. Nowak, T. Porco, P. Sykora, L. Simonsen, J. Spitznagel, R. Tauxe, F. Tenover, Resistance to antimicrobial chemotherapy: a prescription for research and action, Am. J. Med. Sci. 315 (1998) 87–94.
[41] D.J. Austin, R.M. Anderson, Studies of antibiotic resistance within the patient, hospitals and the community using simple mathematical models, Philos. Trans. R. Soc. Lond. B 354 (1999) 721–738.
[42] F.M. Stewart, R. Antia, B.R. Levin, M. Lipsitch, L.E. Mittler, The population genetics of antibiotic resistance II: analytical theory for sustained populations of bacteria in a community of hosts, Theor. Popul. Biol. 53 (1998) 152–165.
[43] D.J. Austin, M. Kakehashi, R.M. Anderson, The transmission dynamics of antibiotic-resistant bacteria: the relationship between resistance in commensal organisms and antibiotic consumption, Proc. R. Soc. Lond. Ser. B 264 (1997) 1629–1638.
[44] B.R. Levin, J.J. Bull, Phage theory revisited: the population biology of a bacterial infection and its treatment with bacteriophage and antibiotics, Am. Nat. 147 (1998) 881–898.
[45] M. Lipsitch, B.R. Levin, Population dynamics of tuberculosis treatment: mathematical models of the roles of noncompliance and bacterial heterogeneity in the evolution of drug resistance, Int. J. Tuberculosis Lung Dis. 2 (1998) 187–199.
[46] M. Lipsitch, B.R. Levin, The population dynamics of antimicrobial chemotherapy, Antimicrob. Agents Chemother. 41 (1997) 363–373.
[47] S.M. Blower, P.M. Small, P.C. Hopewell, Control strategies for tuberculosis epidemics: new models for old problems, Science 273 (1996) 497–500.
[48] E. Massad, S. Lundberg, H.M. Yang, Modeling and simulating the evolution of resistance against antibiotics, Int. J. Biomed. Comput. 33 (1993) 65–81.
[49] E.M. Dougherty, R.M. Weiner, J.L. Vaughn, C.F. Reichelderfer, Physical factors that affect in vitro Autographa californica nuclear polyhedrosis virus infection, Appl. Environ. Microbiol. 41 (1981) 1166–1172.
[50] D.M. Knipe, P.M. Howley, D.E. Griffin, M.A. Martin, B. Roizman, S.E. Straus, Fields' Virology, fifth ed., Lippincott Williams & Wilkins, Philadelphia, 2006.
[51] M.P. Zwart, N. Tromas, S.F. Elena, Model-selection-based approach for calculating cellular multiplicity of infection during virus colonization of multi-cellular hosts, PLos ONE 8 (2013) e64657.
[52] S. Frank, Multiplicity of infection and the evolution of hybrid incompatibility in segmented viruses, Heredity 87 (2001) 522–529.
[53] S. Gutiérrez, M. Yvon, G. Thébaud, B. Monsion, Y. Michalakis, S. Blanc, Dynamics of the multiplicity of cellular infection in a plant virus, PLoS Pathog 6 (2010) e1001113.
[54] J. Maynard Smith, Evolution and the Theory of Games, Cambridge University Press, Cambridge, UK, 1982.
[55] K. Komatsu, S. Okuda, M. Takahashi, R. Matsunaga, Antibiotic effect of insect-resistant soybean on common cutworm (*Spodoptera litura*) and its inheritance, Breeding Sci. 54 (2004) 27–32.
[56] D.R. O'Reilly, L.K. Miller, A baculovirus blocks insect molting by producing ecdysteroid UDP-glucosyl transferase, Science 245 (1989) 1110–1112.

[57] C.J. Funk, S.C. Braunagel, G.F. Rohrmann, Baculovirus structure, in: L.K. Miller (Ed.), The Baculoviruses, Plenum Press, New York, 1997, pp. 7–32.
[58] Y.M. Chen, R.L. Nelson, Variation in early plant height in wild soybean, Crop Sci. 46 (2006) 865–869.
[59] H. McCallum, N. Barlow, J. Hone, How should pathogen transmission be modelled?, Trends Ecol Evol. 16 (2001) 295–300.
[60] G. Dwyer, J.S. Elkinton, J.P. Buonaccorsi, Host heterogeneity in susceptibility and the dynamics of infectious disease: tests of a mathematical model, Am. Nat. 150 (1997) 685–707.
[61] M.A. Nowak, C.R.M. Bangham, Population dynamics of immune responses to persistent viruses, Science 272 (1996) 74–79.
[62] J. Schulze-Horsel, M. Schulze, G. Agalaridis, Y. Genzel, U. Reichl, Infection dynamics and virus-induced apoptosis in cell culture-based influenza vaccine production–Flow cytometry and mathematical modeling, Vaccine 27 (2009) 2712–2722.
[63] F. Van den Bosch, A. Gordon, S. Sue, J. Mike, Host resistance and evolutionary response of plant viruses, J. Appl. Ecol. 43 (2006) 506–516.
[64] A. Chikhalya, D.D. Luu, M. Carrera, A. De La Cruz, M. Torres, E.N. Martinez, T. Chen, K.D. Stephens, E.J. Haas-Stapleton, Pathogenesis of *Autographa californica* multiple nucleopolyhedrovirus in fifth-instar *Anticarsia gemmatalis* larvae, J. Gen. Virol. 90 (2009) 2023–2032.
[65] N.M. Dixit, A.S. Perelson, HIV dynamics with multiple infections of target cells, Proc. Nat. Acad. Sci. USA 102 (2005) 8198–8203.
[66] C.T. Bancroft, T.G. Parslow, Evidence for segment-nonspecific packaging of the influenza a virus genome, J. Virol. 76 (2002) 7133–7139.
[67] P.V. Driessche, J. Watmough, Reproduction numbers and sub-threshold endemic equilibria for compartmental models of disease transmission, Math. Biosci. 180 (2002) 29–48.
[68] M.J. Foxe, W.F. Rochow, Importance of virus source leaves in vector specificity of barley yellow dwarf virus, Phytopathology 65 (1975) 1124–1129.
[69] N.G. Dalal, W.E. Bentley, Mathematical characterization of insect cell (Sf-9) death in suspended culture, Biotechnol. Lett. 21 (1999) 325–329.
[70] S.L. Peck, Antibiotic and insecticide resistance modeling–is it time to start talking?, Trends Microbiol 9 (2001) 286–292.
[71] U.L.F. Dieckmann, J.A.J. Metz, M.W. Sabelis, K. Sigmund, Adaptive Dynamics of Infectious Diseases in Pursuit of Virulence Management, Cambridge University Press, Cambridge, 2002.
[72] R.A. Ball, L.C. Purcell, E.D. Vories, Optimizing soybean plant population for a short-season production system in the southern USA, Crop Sci. 40 (2000) 757–764.
[73] L. Möhler, D. Flockerzi, H. Sann, U. Reichl, Mathematical model of influenza a virus production in large-scale microcarrier culture, Biotechnol. Bioeng. 90 (2005) 46–58.